Protective effect of ulinastatin on severe pulmonary infection under immunosuppression and its molecular mechanism

WENSHUAI LIU*, GUOZHONG PANG*, SHENGYAN WANG and AIQIN SUN

Intensive Care Unit, Dezhou People's Hospital, Dezhou, Shandong 253000, P.R. China

Received May 18, 2017; Accepted August 16, 2017

DOI: 10.3892/etm.2017.4993

Abstract. The objective of the present study was to investigate the protective effect of ulinastatin on severe pulmonary infection under immunosuppression, and its molecular mechanism. Mice were treated with methylprednisolone and lipopolysaccharide (LPS) to establish the model of severe pulmonary infection under immunosuppression. Mice were randomly divided into group A (model group; treated with equal volumes of saline), group B (treated with $1x10^5$ U/kg ulinastatin), and group C (normal control group). Bronchoalveolar lavage fluid (BALF) was collected, and the concentrations of cytokines in BALF were measured by enzyme-linked immunosorbent assay (ELISA). Pathological changes in lung tissues were observed by hematoxylin and eosin (H&E) staining. The mRNA levels of M1 and M2 macrophage markers in lung tissues were detected by real-time polymerase chain reaction (PCR). Specific protein levels in lung tissues were measured by western blotting. Apoptosis in lung tissues was detected by the terminal-deoxynucleoitidyl transferase mediated nick end-labeling (TUNEL) method. The concentrations of TNF-α, IL-6, and IL-1β in BALF, the mRNA levels of the three M1 macrophage markers, and the protein levels of p-Janus Kinase 2 (p-JAK2), p-signal transducer and activator of transcription-3 (p-STAT-3), cleaved caspase-9, and cleaved poly-ADP-ribose polymerase (PARP), and the number of apoptotic cells in lung tissues in group A were significantly higher than those in groups B and C ($P<0.05$), whereas the concentrations of IL-4, IL-10, and IL-13 and the mRNA levels of the three M2 macrophage markers were significantly lower than those in groups B and C ($P<0.05$). Immunofluorescence showed that the nuclei of lung epithelial macrophages in group A became smaller and moved towards the side of nuclear membranes. In conclusion, ulinastatin can improve the inflammatory response caused by severe infection under immunosuppression, which balances the inflammatory microenvironment and inhibits apoptosis at least partially through inhibiting JAK2/STAT-3 and/or caspase pathway activity, ultimately playing a role in lung protection.

Correspondence to: Dr Shengyan Wang, Intensive Care Unit, Dezhou People's Hospital, 1751 Xinhu Street, Dezhou, Shandong 253000, P.R. China
E-mail: vhn8nj@163.com

*Contributed equally

Key words: ulinastatin, immunosuppression, severe infection, inflammatory response, apoptosis

Introduction

Clinical studies have shown that extensive use of immunosuppressors, such as cyclosporine A, methylprednisolone, and glucocorticoids in tumor radiotherapy and chemotherapy, has resulted in continuously increasing numbers of clinically immunosuppressed patients with connective tissue disease, chronic obstructive pulmonary disease, and other diseases. Pulmonary infection caused by immunosuppression is the main cause of death in patients with severe infection, and has attracted clinical attention (1). The use of immunosuppressors can easily result in secondary decreased immunity, enhancing the body's susceptibility to pathogens. Studies have confirmed that the fatality rate associated with bacterial, viral, or fungal infection of the lungs and other organs caused by immunosuppression is as high as 45-90%, and the cause of death is related to excessive systemic inflammation caused by infection (2). Therefore, searching for and developing drugs that can control excessive inflammation under immunosuppression are of great significance for improving the survival of patients with immunosuppressive pulmonary infection.

Ulinastatin is a glycoprotein composed of 143 amino acids, obtained by separation and purification from male urine. It has inhibitory effects on multiple enzymes (3). Studies found that ulinastatin can inhibit the release of inflammatory factors resulting from various causes, and regulate the balance of the inflammatory microenvironment, thus protecting tissues from injury (4,5). Previous studies found that ulinastatin can inhibit the adhesion and aggregation of neutrophils on endothelial cells and the release of substances from endothelial cells or neutrophils, antagonize reactive oxygen free radicals, and enhance immunity (6). Ulinastatin can inhibit the production of lipopolysaccharide (LPS)-induced secretion of tumor necrosis factor-α (TNF-α) and proinflammatory cytokines from monocytes, thus improving immunosuppression (7-9). At present, the detailed molecular mechanism of ulinastatin on the inhibition of the inflammatory response remains unclear, and there are no reports on whether it can regulate the balance of the inflammatory microenvironment under

immunosuppression. In this study, the effects of ulinastatin on pathology, the levels of inflammatory mediators, apoptosis, and macrophage polarization in mice with lung injury were observed. In addition, the organ protective effect and molecular mechanism of ulinastatin under immunosuppression were investigated by establishing an immunocompromised mouse model with severe pulmonary infection.

Materials and methods

Experimental animals. Forty-five C57BL/6 mice (both males and females) aged 6-8 weeks, weighing 26.5±4.8 g, were provided by the Experimental Animal Center of AAA University. Experimental mice were used strictly in accordance with the national animal experimental requirements, and the study was approved by the Animal Management Committee of Dezhou People's Hospital Animal Center. Feeding temperature: 22-25˚C, relative humidity: 55-60%; 12 h illumination, diurnal cycle, free diet and drinking.

Reagents. LPS was from Sigma; methylprednisone was from China Pharmaceutical and Biological Products Testing Center; STAT-3, p-STAT-3, caspase-9, cleaved caspase-9, and cleaved PARP antibodies were from Abcam; horseradish peroxidase-labeled secondary IgG antibody was from Beijing Zhongshan Goldenbridge Biotechnology Co., Ltd.; TNF-α, IL-6, IL-1β, IL-4, IL-10, and IL-13 ELISA kits were from Shanghai Lanpai Biotechnology Co., Ltd.; TUNEL cell apoptosis detection kits were from Maixin Biotechnology Development Co., Ltd.; diaminobenzidine (DAB) staining kits were from Beijing CellChip Biotechnology Co., Ltd.; TRIzol reagents (RNAiso Plus), RPMI-1640 cell culture medium, and reverse transcription reagents (SYBR® Premix Ex Taq™ II) were from Takara; BCA protein concentration detection kits were from Thermo Fisher Scientific, Inc.; other reagents were analytically pure and made in China.

Establishment of the immunosuppressed mouse model with severe pulmonary infection, and grouping. According to previously described methods (10), the immunosuppressed mouse model with severe pulmonary infection was established, and mice were divided into group A (model group, immunosuppressive severe infection group), group B (ulinastatin group), and group C (normal control group). Mice in group A and group B were injected intraperitoneally with methylprednisolone (30 mg/kg) for 3 consecutive days, and received intraperitoneal injection of ulinastatin ($1x10^5$ U/kg) 30 min before and after LPS infection on the 4th day. Mice in the model group were injected with the same volume of normal saline.

Collection of bronchoalveolar lavage fluid (BALF) and determination of inflammatory mediator concentrations. After LPS infection for 6 h, mice were sacrificed under anesthesia, and fixed on an operating plate. The trachea was anatomized, exposed, and ligated. The venous indwelling needle was inserted and fixed in the trachea. A total of 1 ml of RPMI-1640 cell culture medium was poured into the lungs in total three times. BALF was collected in 5 ml centrifuge tubes, followed by centrifugation at 377.325 x g for 10 min, and the supernatant was collected. The concentrations (pg/ml) of TNF-α, IL-6, IL-1β, IL-4, IL-10, and IL-13 in BALF were measured according to the instruction of the ELISA kits.

H&E staining. Lung tissues were separated, and lung tissue samples (3x3 mm) were treated as follows: fixation with 4% paraformaldehyde, paraffin embedding, ethanol dehydration, xylene transparency, dewaxing, embedding, and sectioning (5 μm). According to standard H&E staining methods, tissue sections were treated as follows: xylene dewaxing, gradient ethanol dehydration, hematoxylin staining, ethanol dehydration, eosin staining, and xylene transparency. After sealing with neutral gum, samples were observed and photographed under an optical microscope (BX-42; Olympus, Tokyo, Japan).

Real-time PCR. Total RNA from lung tissue was extracted according to the instructions of the TRIzol kit, and OD values were measured by spectrophotometry. Samples were stored at -80˚C. cDNA was synthesized according to the instructions of the RT-PCR kit. Reaction conditions: 42˚C for 1 h, 70˚C for 5 min. cDNA was placed at 4˚C for 10 min, and stored at -80˚C. Real-time PCR was performed with 2 ng cDNA. The primers used are shown in Table I. Reaction conditions: pre-denaturation at 95˚C for 5 min; 95˚C for 30 sec; 60˚C for 30 sec; 72˚C for 35 sec, for a total of 40 cycles; 72˚C for 10 min. Real-time PCR data analysis was performed using the SYBR Green II fluorescent dye method and the IQ5™ Real-time PCR Detection System (Bio-Rad). The results were normalized to the levels of tubulin, and the relative mRNA levels of M1 markers [IL-6, CD86, and reactive oxygen species (ROS)] and M2 markers (Arg-1, MgI-1 and CD209) are presented as $2^{-\Delta\Delta Ct}$.

Western blotting. A total of 50 mg of lung tissue was treated with 500 μl RIPA (50 mM Tris-HCl pH 7.5, 150 mM NaCl, 1% NP-40, 0.5% sodium deoxycholate, 0.1% SDS), followed by ultrasonic disruption, centrifugation at 10,500 x g and 4˚C for 10 min, and determination of protein concentration by the BCA method. A total of 30 μg of samples was separated by SDS-PAGE. Protein was transferred to PVDF membranes, and blocked with 10% skim milk powder. Membranes were incubated with primary antibodies at 4˚C overnight. Primary rabbit monoclonal STAT-3 antibody (dilution, 1:500; cat. no. ab68153), rabbit monoclonal p-STAT-3 antibody (dilution, 1:500; cat. no. ab219593), rabbit monoclonal caspase-9 antibody (dilution, 1:500; cat. no. ab202068), rabbit monoclonal cleaved caspase-9 antibody (dilution, 1:500; cat. no. ab2324), rabbit monoclonal PARP antibody (dilution, 1:500; cat. no. ab32138), rabbit monoclonal cleaved PARP antibody (dilution, 1:500; cat. no. ab32064) were purchased from Abcam (Cambridge, MA, USA). Membranes were washed, and incubated with secondary goat anti-rabbit (HRP) IgG antibody (dilution, 1:2,000; cat. no. ab6721; Abcam) at room temperature for 1 h, followed by ECL development. The relative protein levels were analyzed by ImageJ software (Media Cybernetics, Silver Springs, MD, USA) after normalization to the internal reference.

Apoptosis. Myocardial apoptosis was analyzed using the TUNEL method according to the instructions of the kit. Left ventricular tissues were dewaxed and dehydrated with ethanol, and 20 μg/ml protein kinase k was added to incubate

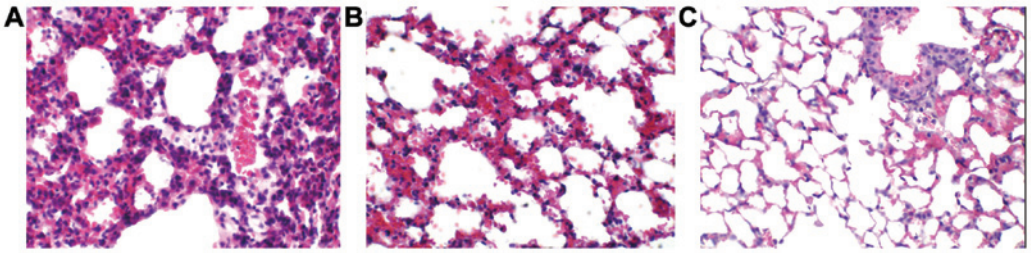

Figure 1. Morphological observation of lung tissues of mice in the different groups (H&E staining, x40). (A) Model group; (B) ulinastatin group; (C) normal control group.

Table I. Real-time PCR primers.

Target gene	Upstream primer (5'-3')	Downstream primer (5'-3')
IL-6	ATTACTGTGCCAGAAACG	TGTGAAGTCTGTCCCTGA
CD86	ATGGGCTCGTATGATTGT	CTTCTTAGGTTTCGGGTG
ROS	ATCCCGTAAGTGTACCTCA	AACCCAAACAAGAATCAGAAGT
Arg-1	AAGACAGCAGAGGAGGTG	TTTGAACAGCGTGGATAT
MgI-1	TGTACGCTGCCTCTACTTTG	CTGTGGCTGCTGGAACCT
CD209	GCTGGAACGACGACAAAT	CACATGGCAACCCAAATA
Tubulin	TTCCAGGACTCCATACCA	CACATCACAGTGTCTTTCG

Table II. Comparisons of cytokine concentrations in BALF in the different groups (mean ± SD, pg/ml).

	M1			M2		
Group	TNF-α	IL-6	IL-1β	IL-4	IL-10	IL-13
A	114.5±22.8[a,b]	134.2±25.4[a,b]	90.6±8.7[a,b]	28.3±3.5[a,b]	18.6±2.4[a,b]	33.8±5.5[a,b]
B	51.4±3.5	61.8±7.2	42.4±3.7	47.32±3.8	36.4±6.0	47.8±6.4
C	45.8±4.0	55.2±9.3	37.1±5.2	52.8±4.2	41.8±7.8	55.0±8.8

Group A, model group; group B, ulinastatin group; group C, normal control group. [a]P<0.05 compared with group C; [b]P<0.05 compared with group B.

the tissues at 37˚C for 15 min. Next, 0.3% H_2O_2 was added to inactivate endogenous oxidases. Tissue sections were washed five times with PBS, and 30 μl TUNEL mixed solution was added to incubate sections at 37˚C for 1 h. Tissue sections were then washed five times with PBS, and 30 μl TUNEL mixed solution was added, followed by staining at 37˚C for 30 min and washing with PBS. Tissues were observed with a Nikon Eclipse 80i biological microscope (Nikon, Tokyo, Japan), and the results were photographed. Nuclei were displayed in blue, and apoptotic cells in red. The apoptotic rate was calculated from observation of five randomly selected visual fields.

Statistical analysis. Data were analyzed using SPSS 17.0 statistical software (SPSS, Inc., Chicago, IL, USA). The results are presented as mean ± standard deviation. The t-test was used for comparisons between two groups. One-way analysis of variance (ANOVA) was used for comparisons among groups. P<0.05 was considered to indicate a statistically significant difference.

Results

Morphological observation. H&E staining results are shown in Fig. 1. Microscopically, pulmonary alveoli, terminal bronchioles, and the entire lung tissue structure were severely damaged in the model group. A large amount of neutrophil and macrophage infiltration was observed in the alveolar cavity, substantial erythrocyte leakage occurred in alveoli, significant infiltration and edema were found in alveoli, and both the alveolar wall and pulmonary interstitium were thickened (Fig. 1A). The structures of most lung tissues in the ulinastatin group remained intact, and the degree of lung injury was alleviated compared with the model group. There was a minimal amount of inflammatory cell infiltration, no erythrocyte leakage, and decreased collapse of alveolar and terminal bronchioles (Fig. 1B). The entire lung tissue structure in the normal group remained intact without congestion, erythrocyte leakage, or inflammatory cell infiltration (Fig. 1C), indicating that ulinastatin can improve the degree of lung injury and play a role in lung protection.

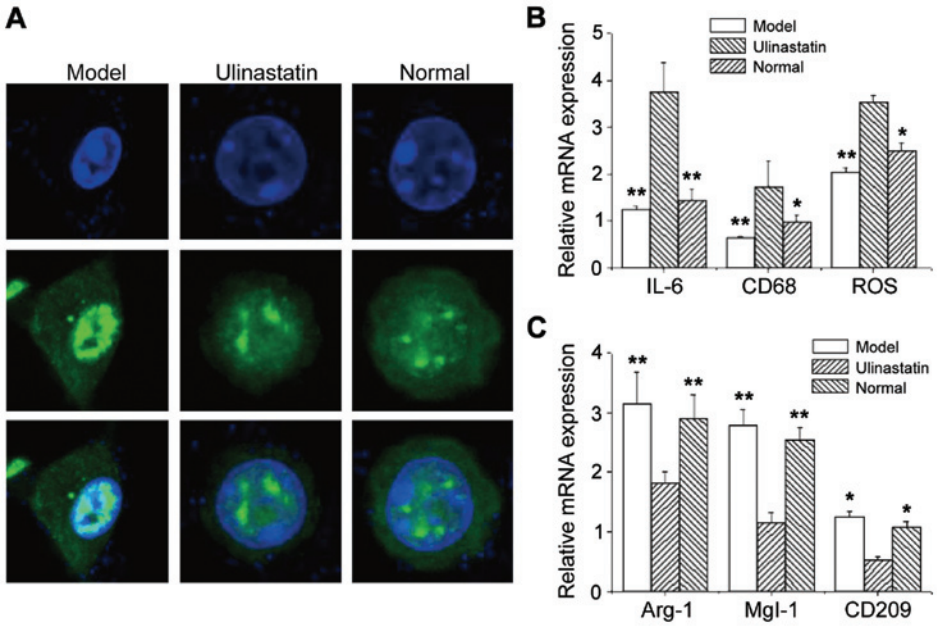

Figure 2. Polarization from M1 macrophages to M2 macrophages induced by ulinastatin. (A) Nuclei of pulmonary epithelial macrophages; (B) mRNA levels of M1 macrophage markers (IL-6, CD68, and ROS); (C) mRNA levels of M2 macrophage markers (Arg-1, MgI-1, and CD209). *P<0.05, **P<0.01 compared with the model group.

Effects of ulinastatin on the concentrations of M1 and M2 inflammatory cytokines. The concentrations of M1 cytokines in BALF of group A were significantly higher than those of group B and group C, and the differences in pairwise comparison were statistically significant (P<0.05) (Table II). In contrast, the concentrations of M2 cytokines in BALF of group A were significantly lower than those of group B and group C. The concentrations of M1 and M2 cytokines in BALF of group B were higher and lower than those in group C, respectively, although the differences were not statistically significant (P>0.05), suggesting that severe pulmonary infection causes inflammation, and ulinastatin can promote the polarization from proinflammatory M1 macrophages to anti-inflammatory M2 macrophages, thereby regulating the inflammatory microenvironment.

Ulinastatin induces polarization from M1 cells to M2 cells. Immunofluorescence showed that the nuclei of pulmonary epithelial macrophages in the model group became smaller and moved towards the side of the nuclear membrane. However, there was no significant change in cell structure in the ulinastatin group compared with the normal control group (Fig. 2A). It is possible that such a change may be related to the functional changes of pulmonary epithelial macrophages. Real-time PCR analysis showed that the mRNA levels of M1 macrophage markers (IL-6, CD68, and ROS) in the model group were significantly higher than those in the ulinastatin group and normal control group (P<0.05) (Fig. 2B). Under the same conditions, the mRNA levels of M2 macrophage markers (Arg-1, MgI-1, and CD209) were significantly lower than those in the ulinastatin group and normal control group (P<0.05) (Fig. 2C). There were no significant differences in the mRNA levels of M1 or M2 macrophage markers between the ulinastatin group and normal control group (Fig. 2B and C). This may be because in acute lung injury caused by severe infection, the expression of proinflammatory cytokines is increased and the expression of anti-inflammatory cytokines is downregulated. Ulinastatin may regulate the balance of the inflammatory microenvironment through polarization from M1 macrophages to M2 macrophages.

Effect of ulinastatin on the JAK2/STAT-3 signaling pathway. Western blot showed that the protein levels of p-JAK2 (1.56±0.25) and p-STAT-3 (1.38±0.32) in lung tissues from the model group were significantly increased (P<0.05). The protein levels of p-JAK2 (0.94±0.14) and p-STAT-3 (0.75±0.11) in the ulinastatin group were significantly lower than those in the model group (P<0.05), but higher than those in group C (p-STAT-3: 0.60±0.08). The protein levels of JAK2 and STAT-3 in lung tissues from the three groups did not change significantly, suggesting that the JAK2/STAT-3 pathway is activated by lung injury caused by severe infection, and ulinastatin can inhibit the activity of the JAK2/STAT-3 pathway in severe lung injury under immunosuppression (Fig. 3).

Effect of ulinastatin on the apoptosis pathway. The levels of cleaved caspase-9 and cleaved PARP in lung tissues from group B and group C were significantly increased (Fig. 4A). The number of apoptotic cells was increased significantly (group B: 14.8±3.4; group C: 11.5±2.7), and the differences were statistically significant compared with group A (35.5±4.6) (P<0.05) (Fig. 4B). There were no significant changes in the levels of caspase-9 and PARP. This suggested that ulinastatin plays a role in lung protection, at least partially through inhibition of apoptosis caused by acute lung injury.

Discussion

Ulinastatin is a urinary trypsin inhibitor obtained by separation and purification from male urine (3). Previous studies found that

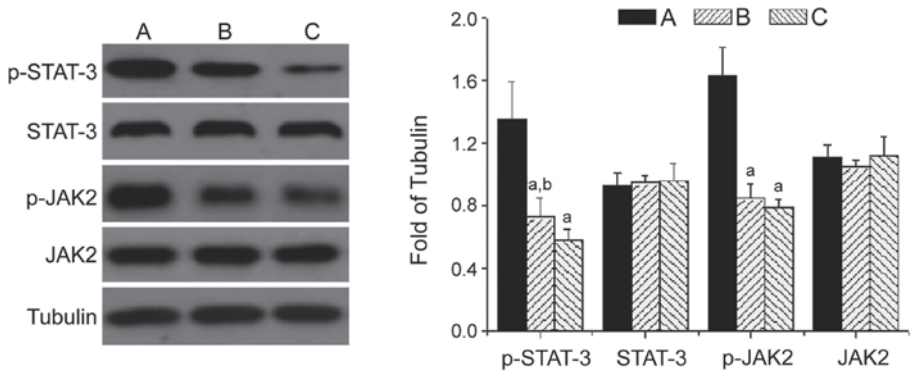

Figure 3. Effect of ulinastatin on the JAK2/STAT-3 signaling pathway. Group A, model group; group B, ulinastatin group; group C, normal control group; [a]P<0.05 compared with group A; [b]P<0.05 compared with group C.

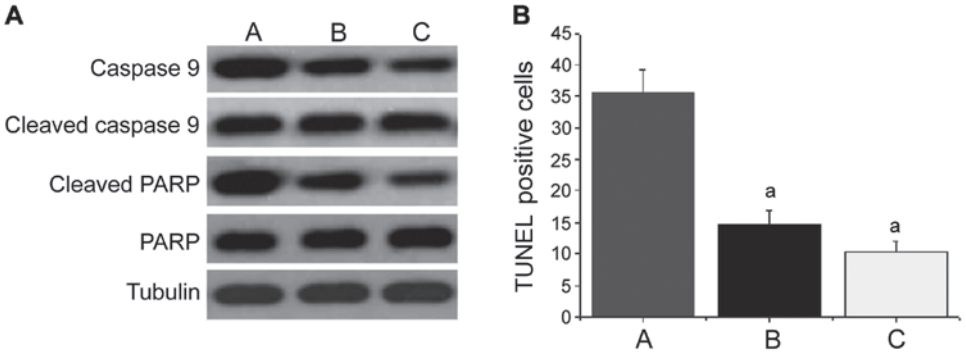

Figure 4. Effect of ulinastatin on apoptotic pathways. (A) Levels of cleaved caspase-9 and cleaved PARP in lung tissues; (B) the number of apoptotic cells. Group A, model group; group B, ulinastatin group; group C, normal control group; [a]P<0.05 compared with group A.

ulinastatin can inhibit the production of inflammatory factors and the release of inflammatory mediators, and improve the imbalance of the inflammatory microenvironment (5,11). The results of this study showed that the lung structure of immunosuppressed mice with severe pulmonary infection was severely damaged, the alveolar wall and pulmonary interstitial distance were increased significantly, terminal bronchioles and alveolar structures were collapsed, and there was substantial erythrocyte leakage and macrophage infiltration. The concentrations of proinflammatory cytokines, IL-6, TNF-α, and IL-1β, in BALF were significantly increased, while the concentrations of anti-inflammatory cytokines, IL-4, IL-10, and IL-13 were significantly decreased, suggesting that severe pulmonary infection under immunosuppression causes imbalance of the inflammatory microenvironment, and the excessive release of proinflammatory factors leads to the inflammatory response, resulting in severe lung injury. The degree of lung injury was significantly improved in the ulinastatin group. The concentrations of anti-inflammatory cytokines, IL-6, TNF-α, and IL-1β, and proinflammatory cytokines, IL-4, IL-10, and IL-13 mostly returned to normal levels, and there were no significant differences compared with the normal control group, indicating that ulinastatin can inhibit the inflammatory response caused by acute lung injury and the balance of the inflammatory microenvironment, which is consistent with previous studies (12,13).

At present, the molecular mechanism of ulinastatin in lung protection through inhibition of inflammation remains unclear. Studies have shown that activated macrophages secrete a large number of inflammatory factors, such as TNF-α, IL-6, IL-12, and IL-18, leading to excessive inflammation in severe bacterial infection, viral infection, and fungal infection in AIDS patients with low immunity (14), indicating that functional activation of macrophages may play an important role in the regulation of proinflammation and anti-inflammation (10). In this study, it was found that the morphology of pulmonary epithelial macrophages in the model group was significantly changed, and nuclei became smaller and moved towards the side of nuclear membranes, suggesting that such a change may be related to the functional activation of these cells. Furthermore, the mRNA levels of M1 macrophage markers (IL-6, CD68, and ROS) were significantly increased, while the mRNA levels of M2 macrophage markers (Arg-1, MgI-1, and CD209) were significantly decreased. There were no significant differences in the mRNA levels of M1 and M2 macrophage markers in the ulinastatin group compared with the control group, suggesting that ulinastatin may regulate the inflammatory microenvironment through polarization from M1 macrophages into M2 macrophages.

Studies found that monocytes, NK cells, $CD8^+$ cells, and Th1 cells secrete the apoptotic factors, TNF-α and FasL, leading to non-cell membrane damage, and inducing a large number of immune cell apoptosis and reducing immune function. In this study, the concentration of TNF-α in BALF, and the levels of cleaved caspase-9 and cleaved PARP in lung tissue from the model group were increased significantly, and the number of apoptotic cells was increased significantly,

suggesting that the apoptotic pathway is activated in severe infection patients with immunosuppression. The concentration of TNF-α in BALF in the ulinastatin group was significantly lower than that in the model group, and the levels of cleaved caspase-9 and cleaved PARP were significantly decreased. Moreover, there were no significant differences compared with the normal control group, indicating that ulinastatin plays a role in lung protection, at least partially through inhibition of apoptosis caused by acute lung injury.

The JAK/STAT pathway is an important intracellular signal transduction pathway. It was found that this pathway is important for the biological function of many cytokines (14,15). Previous studies have shown that activation of the JAK2/STAT-3 pathway plays an important role in the inflammatory response caused by acute lung injury (16-18). In this study, the protein levels of p-JAK2 and p-STAT-3 were significantly increased in lung injury caused by severe infection under immunosuppression, while the protein levels of p-JAK2 and p-STAT-3 in the ulinastatin group were significantly decreased. Additionally, there were no significant differences compared with the normal control group, suggesting that the JAK2/STAT-3 pathway is activated in lung injury caused by severe infection under immunosuppression, imbalance of the inflammatory microenvironment is closely related to the activation of the JAK2/STAT-3 and caspase pathways, and ulinastatin inhibits inflammation and apoptosis by inhibiting the activity of the JAK2/STAT-3 and/or caspase pathways, ultimately playing a role in lung protection. The detailed molecular mechanism require further study.

References

1. Eschenauer GA, Kwak EJ, Humar A, Potoski BA, Clarke LG, Shields RK, Abdel-Massih R, Silveira FP, Vergidis P, Clancy CJ, *et al*: Targeted versus universal antifungal prophylaxis among liver transplant recipients. Am J Transplant 15: 180-189, 2015.
2. Maynard CL, Elson CO, Hatton RD and Weaver CT: Reciprocal interactions of the intestinal microbiota and immune system. Nature 489: 231-241, 2012.
3. Zhang Y, Chen H, Li YM, Zheng SS, Chen YG, Li LJ, Zhou L, Xie HY and Praseedom RK: Thymosin alpha1- and ulinastatin-based immunomodulatory strategy for sepsis arising from intra-abdominal infection due to carbapenem-resistant bacteria. J Infect Dis 198: 723-730, 2008.
4. Liu G and Yang H: Modulation of macrophage activation and programming in immunity. J Cell Physiol 228: 502-512, 2013.
5. Ibáñez B, Heusch G, Ovize M and Van de Werf F: Evolving therapies for myocardial ischemia/reperfusion injury. J Am Coll Cardiol 65: 1454-1471, 2015.
6. Deng M, Pan Y and Zhang B: Effects of thymosin α1 and ulinastatin on immune function in patients with severe sepsis. Shandong Yiyao 47: 19-20, 2007.
7. Fu R, Chen Z, Wang Q, Guo Q, Xu J and Wu X: XJP-1, a novel ACEI, with anti-inflammatory properties in HUVECs. Atherosclerosis 219: 40-48, 2011.
8. Lai KC, Huang AC, Hsu SC, Kuo CL, Yang JS, Wu SH and Chung JG: Benzyl isothiocyanate (BITC) inhibits migration and invasion of human colon cancer HT29 cells by inhibiting matrix metalloproteinase-2/-9 and urokinase plasminogen (uPA) through PKC and MAPK signaling pathway. J Agric Food Chem 58: 2935-2942, 2010.
9. Wallner G, Solecki M, Ziemiakowicz R, Ćwik G, Dyndor P and Maciejewski R: Morphological changes of the pancreas in course of acute pancreatitis during treatment with Ulinastatin. Pol Przegl Chir 85: 114-122, 2013.
10. Weber MS, Prod'homme T, Youssef S, Dunn SE, Rundle CD, Lee L, Patarroyo JC, Stüve O, Sobel RA, Steinman L, *et al*: Type II monocytes modulate T cell-mediated central nervous system autoimmune disease. Nat Med 13: 935-943, 2007.
11. Tanaka R, Fujita M, Tsuruta R, Fujimoto K, Aki HS, Kumagai K, Aoki T, Kobayashi A, Izumi T, Kasaoka S, *et al*: Urinary trypsin inhibitor suppresses excessive generation of superoxide anion radical, systemic inflammation, oxidative stress, and endothelial injury in endotoxemic rats. Inflamm Res 59: 597-606, 2010.
12. Leng YX, Yang SG, Song YH, Zhu X and Yao GQ: Ulinastatin for acute lung injury and acute respiratory distress syndrome: A systematic review and meta-analysis. World J Crit Care Med 3: 34-41, 2014.
13. Fang Y, Xu P, Gu C, Wang Y, Fu XJ, Yu WR and Yao M: Ulinastatin improves pulmonary function in severe burn-induced acute lung injury by attenuating inflammatory response. J Trauma 71: 1297-1304, 2011.
14. Ahmad A, Husain A, Mujeeb M, Khan SA, Najmi AK, Siddique NA, Damanhouri ZA and Anwar F: A review on therapeutic potential of Nigella sativa: A miracle herb. Asian Pac J Trop Biomed 3: 337-352, 2013.
15. Tao X, Sun X, Yin L, Han X, Xu L, Qi Y, Xu Y, Li H, Lin Y, Liu K, *et al*: Dioscin ameliorates cerebral ischemia/reperfusion injury through the downregulation of TLR4 signaling via HMGB-1 inhibition. Free Radic Biol Med 84: 103-115, 2015.
16. Lin FS, Shen SQ, Chen ZB and Yan RC: 17β-estradiol attenuates reduced-size hepatic ischemia/reperfusion injury by inhibition apoptosis via mitochondrial pathway in rats. Shock 37: 183-190, 2012.
17. Wang Y, Wong GT, Man K and Irwin MG: Pretreatment with intrathecal or intravenous morphine attenuates hepatic ischaemia-reperfusion injury in normal and cirrhotic rat liver. Br J Anaesth 109: 529-539, 2012.
18. Freitas MC, Uchida Y, Zhao D, Ke B, Busuttil RW and Kupiec-Weglinski JW: Blockade of Janus kinase-2 signaling ameliorates mouse liver damage due to ischemia and reperfusion. Liver Transpl 16: 600-610, 2010.